

© 2026 the authors. This work has been accepted to IFAC for publication under a Creative Commons Licence CC-BY-NC-ND.

This paper has been accepted for presentation at the 23rd IFAC World Congress, 2026.

arXiv:2605.23333v1 [eess.SY] 22 May 2026

Safety-Assured Arrival Scheduling in Sequential UAM Corridor Sections under Speed and Separation Constraints [★]

Sasinee Pruekprasert^{*} Shinji Nakadai^{**}
Katsuhiko Nishinari^{*}

^{*} *The University of Tokyo, Tokyo, Japan. (e-mail:
spruekprasert@g.ecc.u-tokyo.ac.jp, tknishi@mail.ecc.u-tokyo.ac.jp)*

^{**} *Intent Exchange, Inc., Tokyo, Japan.
(e-mail: nakadai@intent-exchange.com)*

Abstract: This paper presents a safety-assured arrival-scheduling framework for Urban Air Mobility (UAM) corridor operations. We propose an analytical method to compute a sufficient ETA gap at Constrained Waypoints (CWPs) that guarantees longitudinal separation along sequential corridor sections with heterogeneous speed limits. The resulting ETA-gap condition depends on section-specific speed bounds and the required separation distance, providing an efficiently computable rule suitable for integration into future digital ETA-scheduling and air traffic management systems. We show that the computed ETA gap ensures safe separation across all corridor sections under prescribed section travel times and speed limits. Numerical simulations for a decreasing-speed corridor confirm that vehicles coordinated with the proposed mechanism adjust their speeds to maintain the required spacing, avoid potential collisions, and support improved traffic flow compared with unscheduled operations.

Keywords: Urban Air Mobility, UAM corridors, Arrival scheduling, Safety assurance, Air traffic management

1. INTRODUCTION

Urban Air Mobility (UAM) introduces new air traffic management concepts for on-demand and scheduled aerial transportation in metropolitan areas, attracting growing attention from industry, academia, and government (Thipphavong et al., 2018). As demand increases, existing Air Traffic Control (ATC) systems may face capacity challenges under high traffic density (Vascik and Hansman, 2018). At the same time, structured airspace concepts can improve safety but may increase travel delays compared with free-flight operations (Bauranov and Rakas, 2021). It is therefore essential to develop coordination mechanisms that maintain both safety and operational efficiency under these emerging constraints.

To address these challenges, the Federal Aviation Administration (FAA) incorporated UAM corridors into its UAM ConOps (Fontaine, 2023). UAM corridors are reserved airspace volumes managed by designated authorities, such as Providers of Services for UAM (PSUs), who regulate access and performance. These corridors can support applications such as air taxis (Muna et al., 2021), helping to reduce congestion and infrastructure constraints (Wang et al., 2021), and are envisioned for electric Vertical Takeoff and Landing (eVTOL) and powered-lift aircraft within the FAA’s Advanced Air Mobility (AAM) framework.

Prior work has studied UAM corridor design through graph-based congestion models (Wang et al., 2021; Jiang et al., 2022), geometric or layered architectures (Muna et al., 2021), and taxonomies of structured airspace trade-offs (Lee et al., 2023). Asslouj et al. (2024) further extends these concepts to fixed-corridor systems for Unmanned Aircraft Systems (UAS). However, these studies focus mainly on corridor geometry and routing rather than separation conditions for safe inter-vehicle spacing, as envisioned under Digital Flight (Wing et al., 2022).

Conventional airspace-management research has also studied coordinated scheduling and separation assurance, including Integrated Demand Management (Smith et al., 2016), spatiotemporal conflict-free scheduling (Hildum and Smith, 2012), human-in-the-loop comparisons of separation responsibility (Wing et al., 2010), and pre-flight scheduling for AAM operations (Yokoyama et al., 2025). Although these works highlight the value of scheduled-arrival management, they do not address the fine-grained, waypoint-level safety requirements for high-density UAM corridors.

Building on this foundation, this work extends the ETA-based safety framework to sequences of corridor sections, each with distinct speed bounds that may increase or decrease along the route. Such multi-section configurations naturally arise in realistic UAM operations due to changes in altitude layers, airspace policies, and local traffic densities. Unlike the single-section setting in (Pruekprasert and Nakadai, 2025), heterogeneous speed limits introduce

[★] This work is based on results obtained from a project, JPNP22002, commissioned by the New Energy and Industrial Technology Development Organization (NEDO).

new challenges: a safe ETA gap computed for one section may no longer preserve separation after vehicles transition into an adjacent section with different constraints, and maintaining safety must account for the possibility that vehicles occupy different sections at the same time. To address these issues, our main contributions are:

- extending ETA-based coordination to sequential corridor sections with heterogeneous speed limits;
- constructing conservative spatiotemporal bounds that enclose all admissible trajectories under prescribed section travel times and speed limits;
- reducing the safe ETA-gap computation to checking a finite set of critical times induced by the trajectory-bound critical points; and
- complementing the theoretical results with numerical validation of the computed ETA gaps in a decreasing-speed corridor with downstream traffic compression.

Our method provides efficiently computable temporal-separation conditions that reduce the need for the complex optimization required in (Pruekprasert and Nakadai, 2025) and remain scalable for multi-section UAM ETA management. The computed ETA gap can therefore be incorporated as a safety constraint in broader ETA-scheduling and traffic-management systems.

The remainder of this paper is organized as follows. Section 2 introduces the UAM corridor setting and formulates the safe ETA-gap problem. Section 3 derives conservative spatiotemporal bounds under corridor speed limits, and Section 4 uses these bounds to construct a computationally efficient guaranteed-safe ETA gap. Section 5 presents numerical simulations. Section 6 presents the conclusion.

2. UAM CORRIDOR WITH ETAS AT CWPS

We consider Air Traffic Control (ATC) for inter-vehicle self-separation in Urban Air Mobility (UAM) corridors using shared Estimated Times of Arrival (ETAs) at Constrained Waypoints (CWPs). As illustrated in Fig. 1, CWPs partition the airspace into multiple corridor sections. Each section may reserve specific airspace for different flight phases, and CWPs connect these sections to form an integrated UAM corridor network.

2.1 Vehicle Kinematics and Corridor Constraints

We consider n aerial vehicles, indexed by $i \in \{0, \dots, n-1\}$, entering the corridor in order. Vehicle motion within is modeled as one-dimensional and governed by

$$\dot{x}_i(t) = v_i(t), \quad \dot{v}_i(t) = a_i(t), \quad (1)$$

where $x_i(t)$ and $v_i(t)$ denote the position and speed of vehicle i , and $a_i(t)$ is its acceleration input at time t .

We consider m sequential corridor sections indexed by $j \in 0, \dots, m-1$, where each section j connects CWP $_j$ and CWP $_{j+1}$. For each section j , we specify speed limits $v_{min,j}$ and $v_{max,j}$ representing the operational bounds imposed by the corridor design or airspace regulations. Accordingly, while vehicle i is within section j , its speed must satisfy

$$0 < v_{min,j} \leq v_i(t) \leq v_{max,j}. \quad (2)$$

We also assume consecutive speed-limit intervals overlap, i.e., $[v_{min,j}, v_{max,j}] \cap [v_{min,j+1}, v_{max,j+1}] \neq \emptyset$, so vehicles can adjust speeds when transitioning between sections.

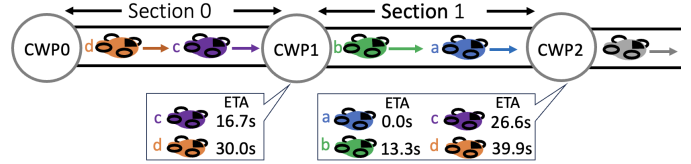


Fig. 1. A UAM corridor network with ETAs at CWPs.

To simplify ETA scheduling, we assign all vehicles a common travel time in each corridor section j to be $\tau_j = \frac{l_j}{v_{avg,j}}$, where $v_{avg,j} = (v_{min,j} + v_{max,j})/2$ is a representative average speed and l_j is the section length. The framework, however, can be extended to heterogeneous travel times.

2.2 Problem Formulation

According to Near Mid-Air Collision (NMAC) avoidance rules, a minimum separation distance is required to ensure safety between aerial vehicles, typically set to a fixed length (Johnson et al., 2017; Muna et al., 2021). We adopt this separation distance as the safety constraint for ETA scheduling at CWPs, requiring that the spacing between vehicles never falls below $safeD$, and formulate the problem of finding a safe ETA gap $\Delta t_{i,i+1}$ as follows.

Problem 1. For two consecutive vehicles i and $i+1$ entering the corridor network in order at CWP $_0$, find

$$\Delta t_{i,i+1} := t_{i+1,enter} - t_{i,enter} > 0$$

such that $x_i(t) - x_{i+1}(t) \geq safeD$,

$$\text{for all } t \in [t_{i+1,enter}, t_{i,enter} + \tau_0 + \tau_1 + \dots + \tau_{m-1}],$$

where $t_{i,enter}$ and $t_{i+1,enter}$ are the entry times at CWP $_0$ if vehicle i and $i+1$, respectively, and $safeD$ is the NMAC minimum separation distance.

Note that because the travel times $\tau_0, \tau_1, \dots, \tau_{m-1}$ are fixed, an ETA gap $\Delta t_{i,i+1}$ at CWP $_0$ also induces ETA gaps $\Delta t_{i,i+1} + \tau_0 + \tau_1 + \dots + \tau_{j-1}$ at each CWP $_j$.

A trivial solution to Problem 1 is to choose $\Delta t_{i,i+1} > \tau_0 + \tau_1 + \dots + \tau_{m-1}$, which ensures that vehicle $i+1$ enters the corridor at CWP $_0$ after vehicle i has exited at CWP $_m$. For example, for the corridor in Fig. 2, this trivial solution requires $\Delta t_{i,i+1} > \tau_0 + \tau_1 + \tau_2 + \tau_3 = 42.1$ s. Although always safe, this choice is excessively conservative. We therefore aim for the smallest $\Delta t_{i,i+1}$ that still guarantees $x_i(t) - x_{i+1}(t) \geq safeD$ for all admissible trajectories.

In the next section, we propose a computationally efficient method to compute a sufficient ETA gap. Although this gap is not necessarily the globally minimal ETA gap, it is guaranteed to satisfy the safety condition in Problem 1 and is typically much smaller than the trivial bound above.

3. SPATIOTEMPORAL TRAJECTORY BOUNDS

To compute a sufficient ETA gap for Problem 1, we first construct conservative spatiotemporal bounds on vehicle trajectories, based on the corridor speed limits. These bounds enable a computationally efficient method for deriving a guaranteed-safe ETA gap in the next section.

Given that all vehicles operate within the speed range $[v_{min,j}, v_{max,j}]$ and spend τ_j time in each corridor section j , their admissible spatiotemporal trajectories are

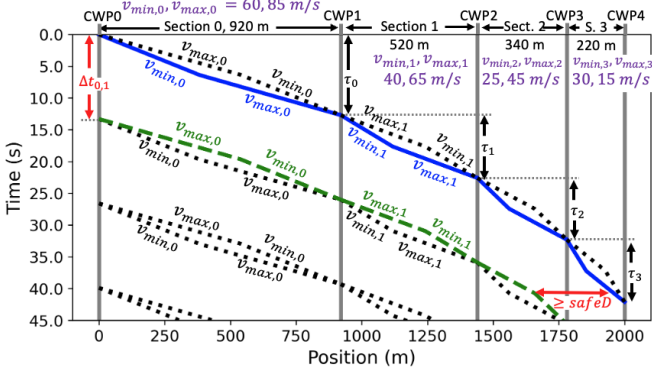


Fig. 2. Conservative spatiotemporal bounds of vehicles trajectories in UAM corridors with $\Delta t_{i,i+1} = 13.3$ s for $\text{safeD} = 300$ m. Length of corridors 0-3: 920, 520, 340, and 220 m; Speed limits: $v_{\min,0} = 60$, $v_{\max,0} = 85$; $v_{\min,1} = 40$, $v_{\max,1} = 65$; $v_{\min,2} = 25$, $v_{\max,2} = 45$; $v_{\min,3} = 15$, $v_{\max,3} = 30$ m/s. Travel times: $\tau_0 = 12.7$, $\tau_1 = 9.9$, $\tau_2 = 9.7$, $\tau_3 = 9.8$ s.

bounded by the slopes as shown in Fig. 2. These bounds arise from two extreme speed profiles: one that switches from $v_{\min,j}$ to $v_{\max,j}$ (blue solid line for vehicle 0 in Fig. 2) and one that switches from $v_{\max,j}$ to $v_{\min,j}$ (green dashed line for vehicle 1), assuming instantaneous speed changes.

Formally, let l_j denote the length of corridor section $j \in \{0, 1, \dots, m-1\}$, and let CWP_0 be located at position 0. We define the cumulative time and position offsets as

$$L_j := \sum_{\ell=0}^{j-1} l_\ell \quad \text{and} \quad T_{i,j} := t_{i,\text{enter}} + \sum_{\ell=0}^{j-1} \tau_\ell, \quad (3)$$

for $j \in \{1, 2, \dots, m\}$, with $L_0 = 0$ and $T_{i,0} = t_{i,\text{enter}}$. Hence, L_j is the position of CWP_j and $T_{i,j}$ is the scheduled time at which vehicle i arrives at CWP_j .

For each corridor section j , define \check{t}_j as the unique non-negative solution of

$$v_{\min,j} \check{t}_j + v_{\max,j} (\tau_j - \check{t}_j) = l_j, \quad (4)$$

representing the switching time of a trajectory that first flies at $v_{\min,j}$ and then at $v_{\max,j}$. Note that such a solution exists if $v_{\min,j} \tau_j \leq l_j \leq v_{\max,j} \tau_j$, which is assumed throughout. For $t \in [T_{i,j}, T_{i,j+1}]$, the trajectory $\check{x}_i(t)$ is

$$\check{x}_i(t) = \begin{cases} L_j + v_{\min,j}(t - T_{i,j}), & \text{if } T_{i,j} \leq t \leq T_{i,j} + \check{t}_j, \\ L_j + v_{\min,j} \check{t}_j + v_{\max,j}(t - T_{i,j} - \check{t}_j), & \text{if } T_{i,j} + \check{t}_j \leq t \leq T_{i,j+1}. \end{cases} \quad (5)$$

Similarly, define \hat{t}_j as the unique nonnegative solution of

$$v_{\max,j} \hat{t}_j + v_{\min,j} (\tau_j - \hat{t}_j) = l_j, \quad (6)$$

corresponding to a trajectory that first flies at $v_{\max,j}$ and then $v_{\min,j}$. The trajectory $\hat{x}_i(t)$ is defined analogously by swapping $v_{\min,j}$ and $v_{\max,j}$, and replacing \check{t}_j with \hat{t}_j in (5).

We now show that these two trajectories bound all admissible motions of a vehicle that satisfy the speed limits (2) and the prescribed section travel times τ_j .

Theorem 1. Consider any vehicle i that satisfies the speed limits condition (2), and spends τ_j time units in

each corridor section $j \in \{0, \dots, m-1\}$. Then, for all $t \in [T_{i,0}, T_{i,m}]$, the vehicle position $x_i(t)$ satisfies

$$\check{x}_i(t) \leq x_i(t) \leq \hat{x}_i(t),$$

i.e., every admissible trajectory lies between the two extreme spatiotemporal bounds.

Proof. Fix a corridor section j and consider any admissible trajectory $x_i(t)$ that satisfies the speed bounds (2) and the fixed travel time τ_j . Let t^* be any time such that vehicle i is flying in corridor section j , and define $x^* := x_i(t^*)$. Then, we have $t^* \in [T_{i,j}, T_{i,j+1}]$ and $x^* \in [L_j, L_{j+1}]$. To prove the theorem, it suffices to show that x^* lies between the lower and upper bounds $\check{x}_i(t^*)$ and $\hat{x}_i(t^*)$.

Assume, for the sake of contradiction, that either $x^* < \check{x}_i(t^*)$ or $\hat{x}_i(t^*) < x^*$. We treat only the former case, as the latter follows symmetrically. Suppose $x^* < \check{x}_i(t^*)$, and let \check{t}_j be the speed-switching time in (4).

If $t^* \leq T_{i,j} + \check{t}_j$, then from (5), we have $\check{x}_i(t^*) = L_j + v_{\min,j}(t^* - T_{i,j})$. Since $x^* < \check{x}_i(t^*)$, we obtain

$$\frac{x^* - L_j}{t^* - T_{i,j}} < \frac{\check{x}_i(t^*) - L_j}{t^* - T_{i,j}} = v_{\min,j},$$

implying an average speed strictly below $v_{\min,j}$ from $(L_j, T_{i,j})$ to (x^*, t^*) , contradicting (2).

Otherwise, $t^* > T_{i,j} + \check{t}_j$. From the second case of (5),

$$\check{x}_i(t^*) = L_j + v_{\min,j} \check{t}_j + v_{\max,j}(t^* - T_{i,j} - \check{t}_j).$$

Using $L_{j+1} = L_j + v_{\min,j} \check{t}_j + v_{\max,j}(\tau_j - \check{t}_j)$ and $T_{i,j+1} = T_{i,j} + \tau_j$, this expression can be rewritten as

$$\check{x}_i(t^*) = L_{j+1} - v_{\max,j}(T_{i,j+1} - t^*).$$

Since $x^* < \check{x}_i(t^*)$, we obtain

$$L_{j+1} - x^* > L_{j+1} - \check{x}_i(t^*) = v_{\max,j}(T_{i,j+1} - t^*),$$

which requires an average speed strictly above $v_{\max,j}$ from (x^*, t^*) to $(L_{j+1}, T_{i,j+1})$, contradicting (2).

As neither case is possible, $\check{x}_i(t^*) \leq x^* \leq \hat{x}_i(t^*)$ for all t^* in section j . Since T_j and L_j accumulate across sections, the bound holds over the entire corridor network. \square

Remark 1. The bounds in Theorem 1 apply to admissible trajectories satisfying the section speed limits and prescribed section travel times. Additional jerk, actuator, or transition-dynamics limits preserve the safety argument if the realized trajectories remain within these bounds. If such constraints or ETA-tracking errors change the realized CWP times, the ETA schedule should be recomputed or enlarged by a timing buffer, e.g., a $\pm \varepsilon$ ETA error at CWP_0 can be handled by adding 2ε to the ETA gap.

4. COMPUTING A SUFFICIENT ETA GAP

This section derives a computationally efficient sufficient ETA gap. By Theorem 1, $\check{x}_i(t)$ lower-bounds the leader trajectory and $\hat{x}_{i+1}(t)$ upper-bounds the follower trajectory. Therefore, $\check{x}_i(t) - \hat{x}_{i+1}(t)$ lower-bounds their separation, yielding the following sufficient condition.

Lemma 1. Consider two consecutive vehicles i and $i+1$ satisfying the speed-limit condition (2) and spending τ_j time units in each corridor section $j \in \{0, \dots, m-1\}$. Let $\Delta t_{i,i+1} = T_{i+1,0} - T_{i,0}$ denote their ETA gap at CWP_0 . If

$$\check{x}_i(t) - \hat{x}_{i+1}(t) \geq \text{safeD}, \quad \forall t \in [T_{i+1,0}, T_{i,m}], \quad (7)$$

then $\Delta t_{i,i+1}$ is a feasible solution of Problem 1.

Proof. By Theorem 1, for all $t \in [T_{i+1,0}, T_{i,m}]$, $x_i(t) \geq \check{x}_i(t)$ and $x_{i+1}(t) \leq \hat{x}_{i+1}(t)$. Hence,

$$x_i(t) - x_{i+1}(t) \geq \check{x}_i(t) - \hat{x}_{i+1}(t) \geq \text{safe}D.$$

Therefore, the condition in Problem 1 holds. \square

Next, we compute the smallest ETA gap satisfying (7). To do so, we extract the *critical points* of the trajectory bounds $\check{x}_i(t)$ and $\hat{x}_{i+1}(t)$, which correspond to the times at which the slope changes. Let \check{C}_i and \hat{C}_{i+1} denote these sets of critical points, defined as follows:

$$\check{C}_i := \bigcup_{j=0}^{m-1} \left\{ (L_j, T_{i,j}), (L_j + v_{\min,j} \check{t}_j, T_{i,j} + \check{t}_j), (L_{j+1}, T_{i,j+1}) \right\},$$

$$\hat{C}_{i+1} := \bigcup_{j=0}^{m-1} \left\{ (L_j, T_{i+1,j}), (L_j + v_{\max,j} \hat{t}_j, T_{i+1,j} + \hat{t}_j), (L_{j+1}, T_{i+1,j+1}) \right\},$$

where \check{t}_j and \hat{t}_j are the unique nonnegative solutions of (4) and (6), respectively

For a given pair of vehicles i and $i+1$, we collect all time instants at which either trajectory bound changes slope. Define the set of relevant time instants as

$$\tilde{T}_i := \{t : \exists x, (x, t) \in \check{C}_i \cup \hat{C}_{i+1}\} \cap [T_{i+1,0}, T_{i,m}]. \quad (8)$$

The following theorem states that (7) can be ensured by checking the separation only at the time instants in \tilde{T}_i .

Theorem 2. Given a pair of vehicles i and $i+1$ and a safety distance $\text{safe}D \geq 0$.

If $\check{x}_i(t) - \hat{x}_{i+1}(t) \geq \text{safe}D$ for all $t \in \tilde{T}_i$,

Then $\check{x}_i(t) - \hat{x}_{i+1}(t) \geq \text{safe}D$ for all $t \in [T_{i+1,0}, T_{i,m}]$.

Proof. Let $d(t) := \check{x}_i(t) - \hat{x}_{i+1}(t)$. From (5), both bounds $\check{x}_i(t)$ and $\hat{x}_{i+1}(t)$ are continuous piecewise-affine functions whose slope changes only at the critical times in \tilde{T}_i . Hence, $d(t)$ is also continuous and affine on each interval between consecutive elements of \tilde{T}_i . Order the elements of \tilde{T}_i as $T_{i+1,0} = t_0 < t_1 < \dots < t_K = T_{i,m}$. On each interval $[t_k, t_{k+1}]$, the function $d(t)$ is affine and thus attains its minimum at one of the endpoints. By the assumption of the theorem, $d(t_k) \geq \text{safe}D$ for all k , which implies $d(t) \geq \text{safe}D$ for all $t \in [t_k, t_{k+1}]$. Taking the union over all intervals yields $d(t) \geq \text{safe}D$ for all $t \in [T_{i+1,0}, T_{i,m}]$, which proves the claim. \square

By Lemma 1 and Theorem 2, it suffices to enforce the separation constraint at the critical times in \tilde{T}_i . This yields the following finite-dimensional optimization problem.

Problem 2. (Reduced ETA-Gap Optimization).

$$\begin{aligned} & \min_{\Delta t_{i,i+1} \in [0, \sum_{j=0}^{m-1} \tau_j]} \Delta t_{i,i+1} \\ & \text{subject to } \check{x}_i(t) - \hat{x}_{i+1}(t) \geq \text{safe}D, \quad \forall t \in \tilde{T}_i, \\ & \quad T_{i+1,0} - T_{i,0} = \Delta t_{i,i+1}. \end{aligned}$$

Remark 2. Since all vehicles are assumed to share the same travel time τ_j in each corridor section j , the resulting minimum ETA gap $\Delta t_{i,i+1}$ is the same for all consecutive

pairs. We nevertheless formulate Problem 2 for a generic pair $(i, i+1)$ to highlight that the method naturally extends to heterogeneous section travel times across vehicles.

Combining Theorem 2 with Lemma 1 yields the following conclusion.

Corollary 1. Consider two consecutive vehicles i and $i+1$ satisfying the speed-limit condition (2) and spending τ_j time units in each corridor section $j \in \{0, \dots, m-1\}$. Let $\Delta t_{i,i+1} = T_{i+1,0} - T_{i,0}$ denote their ETA gap at CWP₀. If $\Delta t_{i,i+1}$ is a solution of Problem 2, then $\Delta t_{i,i+1}$ is a feasible solution of Problem 1. In particular, it guarantees

$$x_i(t) - x_{i+1}(t) \geq \text{safe}D, \quad \forall t \in [T_{i+1,0}, T_{i,m}].$$

Thus, using this ETA gap ensures that all vehicles remain at least $\text{safe}D$ apart for all admissible trajectories.

Remark 3. Corridor lengths and speed limits strongly affect the minimum ETA gap $\Delta t_{i,i+1}$. For instance, setting all corridor section lengths in Fig. 2 to 500 m increases the gap to 16.5 s, compared with 13.3 s in the current setting. This observation suggests that the ETA-gap computation can also serve as a corridor-design evaluation tool. We leave systematic sensitivity analysis over corridor lengths and speed-limit profiles for future work.

Computation procedure. We end this section by summarizing the procedure for computing a sufficient ETA gap. For a given safety distance $\text{safe}D$, the steps for each vehicle pair $(i, i+1)$ are:

- (1) Compute the scheduled CWP times $T_{i,j}$ from the section travel times τ_j for all corridor sections j .
- (2) Construct the spatiotemporal trajectory bounds $\check{x}_i(t)$ and $\hat{x}_{i+1}(t)$ using (5) and its max-to-min counterpart.
- (3) Form the critical-time set \tilde{T}_i from the critical points of the two trajectory bounds as in (8).
- (4) Solve Problem 2, i.e., find the smallest $\Delta t_{i,i+1}$ such that $\check{x}_i(t) - \hat{x}_{i+1}(t) \geq \text{safe}D$ for all $t \in \tilde{T}_i$.

By Corollary 1, the resulting ETA gap $\Delta t_{i,i+1}$ guarantees the required separation for all admissible trajectories.

5. EXPERIMENTAL RESULT

We validate the theoretical results through numerical simulation, comparing operations with and without the proposed ETA gaps. We choose a decreasing-speed corridor as a challenging test case because downstream speed reduction can cause traffic compression and increase collision risk, e.g., when vehicles approach a vertiport. All simulations are implemented in Python 3.12 with a discrete-time step of $\delta_t = 0.1$ s. We use the corridor illustrated in Fig. 2, with $\text{safe}D$ values ranging from 100 m to 1200 m to assess performance under varying spacing requirements.

Vehicle motion follows the discrete-time version of (1):

$$x_i(k+1) = x_i(k) + \delta_t v_i(k), \quad v_i(k+1) = v_i(k) + \delta_t a_i(k).$$

For the first vehicle $i = 0$, while it is in section j , the acceleration is chosen to reduce the difference between its current speed and the average speed required to traverse the section: $a_0(k) = l_j/\tau_j - v_0(k)$. For each following vehicle $i > 0$, inter-vehicle interactions are modeled using

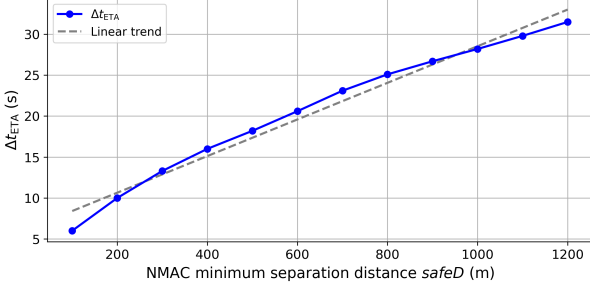


Fig. 3. Relationship between $safeD$ and $t_{i,i+1}$.

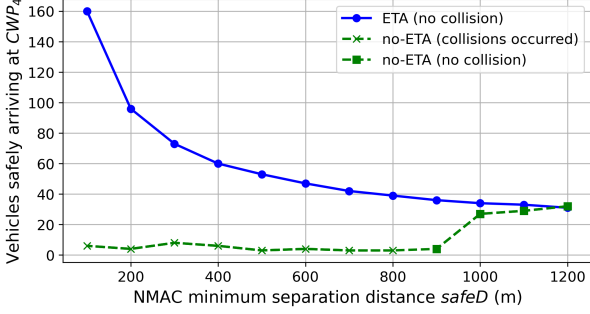


Fig. 4. Number of vehicles that safely arrived at CWP₄.

the Helly vehicle-following model (Helly, 1959; Ambrosio-Lázaro et al., 2018; Li et al., 2024):

$$a_i(k) = \lambda_x(\Delta x - D(v_i(k))) + \lambda_v \Delta v,$$

where $\Delta x = x_{i-1}(k) - x_i(k)$, $\Delta v = v_{i-1}(k) - v_i(k)$, and

$$D(v_i(k)) = D_{\min} + T_{\text{des}}v_i(k)$$

is the desired spacing, with minimum distance D_{\min} and dynamic spacing $T_{\text{des}}v_i(k)$. All accelerations are adjusted as needed to keep speeds within $[v_{\min,j}, v_{\max,j}]$, and clipped to $[-3, 2]$ m/s², which are used as admissible acceleration bounds in the simulation. We consider parameter values $\lambda_x = 0.7$, $\lambda_v = 0.5$, $T_{\text{des}} = 1.2$ s, and vary $D_{\min} = safeD \in \{100, 200, \dots, 1200\}$ m. The values of λ_x , λ_v , and T_{des} follow (Li et al., 2024).

We consider continuous vehicle entry over a 100 s interval. All vehicles enter the network at CWP₀ with an initial speed of 82.5 m/s. Two operation modes are evaluated:

1) *Without ETA gaps (no-ETA)*: Vehicles select their accelerations as described above. The first vehicle enters at time zero, and vehicles $i > 0$ enter the corridor network at CWP₀ as soon as the resulting accelerations are positive.

2) *With ETA gaps (ETA)*: Vehicles follow the same acceleration policy as in the no-ETA case, with additional adjustments when needed to match the section travel times $\tau_0, \tau_1, \dots, \tau_{m-1}$. The first vehicle enters at time zero, and each following vehicle enters at CWP₀ according to the minimum ETA-gap computed by solving Problem 2.

Simulation Results and Analysis.

We solve the optimization Problem 2 for various values of $safeD$. Across all tested values, the minimum ETA gap $\Delta t_{i,i+1}$ is computed in under 0.003 s on a MacBook Pro (M4 Max, 64 GB) using the SciPy function `scipy.optimize.minimize_scalar`. The resulting ETA

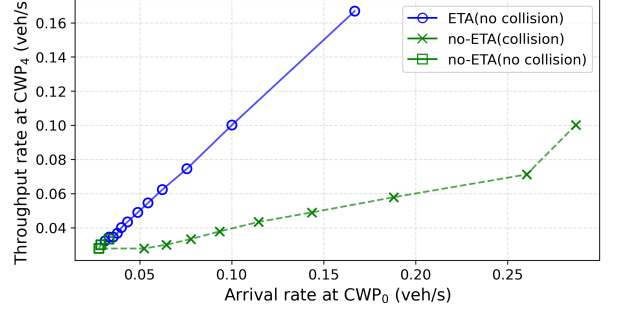


Fig. 5. Vehicle arrival rate at CWP₀ versus the throughput rate at CWP₄.

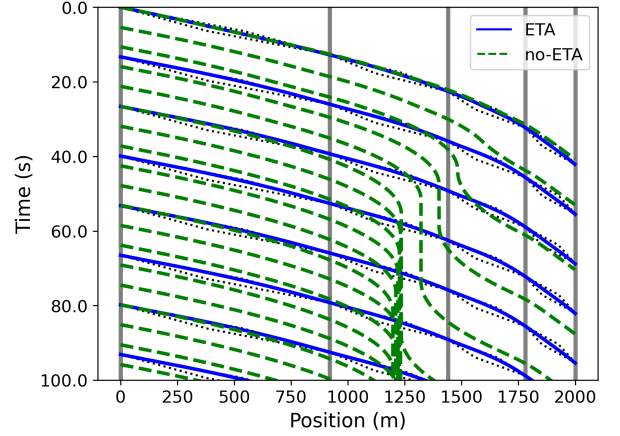


Fig. 6. Spatiotemporal trajectories of vehicles in UAM corridors for $safeD = 300$ m, under the two operation modes: with and without ETA gaps.

gaps for $safeD = 100, 200, \dots, 1200$ m are 6.0, 10.0, 13.3, 16.0, 18.2, 20.6, 23.1, 25.1, 26.7, 28.2, 29.8, and 31.5 s, respectively. As shown in Fig. 3, the required ETA gap increases monotonically with $safeD$, with growth gradually diminishing for larger values.

Figure 4 shows the relation between $safeD$ and the number of vehicles that successfully exit the corridor network at CWP₄ without collision. The ETA-gap policy prevents all collisions for the entire range of $safeD$ considered, even for $safeD = 100$ m. In contrast, the no-ETA mode experiences collisions for all cases with $safeD \leq 800$ m. For the ETA-gap mode, the number of vehicles that complete the full corridor network within the simulation horizon (100 s) decreases as $safeD$ increases, which is expected because larger separation distances require larger ETA gaps at entry. Nevertheless, for all $safeD \leq 1100$ m, the ETA-gap mode allows more vehicles to exit safely than the no-ETA mode. Figure 5 shows the arrival rate at CWP₀ versus the throughput rate at CWP₄. The ETA-gap mode achieves a nearly linear throughput increase, while the no-ETA mode saturates early and remains much lower. Thus, ETA-based coordination improves both safety and flow. Moreover, across all simulations, every vehicle operating with ETA-gap remains at least $safeD$ apart at all times.

Figure 6 shows example spatiotemporal trajectories with and without ETA gaps for $safeD = 300$ m. Vehicles operating under the ETA-gap policy exhibit smooth, uniform flow: their trajectories follow the bounds $\tilde{x}_i(t)$ and $\hat{x}_i(t)$. In

contrast, vehicles in the no-ETA mode experience reactive braking as they approach sections with reduced speed limits, resulting in congestion and, eventually, collisions.

These results show that the ETA-gap mechanism preserves safe inter-vehicle separation while substantially improving traffic flow compared to the unscheduled (no-ETA) mode.

6. CONCLUSION

We presented a computationally lightweight framework for safety-assured arrival scheduling in sequential UAM corridors. By coordinating ETAs at CWPs, we derived a sufficient ETA-gap rule that guarantees inter-vehicle separation across corridor sections with heterogeneous speed limits using conservative spatiotemporal bounds. Numerical simulations confirmed that the ETA-gap policy maintained the required spacing in all scenarios, whereas unscheduled operations experienced congestion and collisions. These findings demonstrate that ETA coordination can improve safety and flow stability in UAM corridors.

These results provide a basis for further developing ETA-based coordination for UAM corridor operations. Future work will consider additional separation criteria, corridor-design strategies, alternative admission policies, ETA-tracking uncertainty, and merging traffic. Other interesting future directions include higher-fidelity vehicle dynamics, mixed speed-profile corridors, and sensitivity studies of vehicle-following parameters and corridor configurations.

ACKNOWLEDGMENT

During the preparation of this work, the authors used ChatGPT-5.4 to support grammar, spelling checks, and wording refinement. After using this tool/service, the authors reviewed and edited the content as needed and takes full responsibility for the content of the publication.

REFERENCES

- Ambrosio-Lázaro, R.C., Quezada-Téllez, L.A., and Rosas-Jaimes, O.A. (2018). Parameter identification on Helly’s car-following model. In *Proc. of 5th International Conference of Control, Dynamic Systems, and Robotics (CDSR’18)*, 107.
- Asslouj, A.E., Uppaluru, H., Ramezani, M., Atkins, E., and Rastgoftar, H. (2024). A fixed air corridor model for UAS traffic management in urban areas. *IEEE Transactions on Aerospace and Electronic Systems*, 60(5), 5651–5662.
- Bauranov, A. and Rakas, J. (2021). Designing airspace for urban air mobility: A review of concepts and approaches. *Progress in Aerospace Sciences*, 125, 100726.
- Fontaine, P. (2023). Urban air mobility concept of operations v2.0. Federal Aviation Administration, Office of NextGen. URL https://www.faa.gov/sites/faa.gov/files/Urban%20Air%20Mobility%20%28UAM%29%20Concept%20of%20Operations%202.0_1.pdf. Accessed: 2026-05-15.
- Helly, W. (1959). Simulation of bottlenecks in single lane traffic flow. In *Proc. of Symposium on Theory of Traffic Flow*, 207–238. Elsevier, New York.
- Hildum, D.W. and Smith, S.F. (2012). Scheduling safe movement of air traffic in crowded air spaces. *The Knowledge Engineering Review*, 27(3), 309–331.
- Jiang, X., Peng, X., Bulusu, V., Poliziani, C., Chatterji, G., and Sengupta, R. (2022). A metrics-based method for evaluating corridors for urban air mobility operations. In *Proc. of 2022 IEEE International Smart Cities Conference (ISC2)*, 1–7.
- Johnson, S.C., Petzen, A., and Tokotch, D. (2017). Exploration of detect-and-avoid and well-clear requirements for small UAS maneuvering in an urban environment. In *Proc. of 17th AIAA Aviation Technology, Integration, and Operations Conference*, 3074.
- Lee, U.J., Ahn, S.J., Choi, D.Y., Chin, S.M., and Jang, D.S. (2023). Airspace designs and operations for UAS traffic management at low altitude. *Aerospace*, 10(9), 737.
- Li, H., Roncoli, C., and Ju, Y. (2024). A Helly model-based MPC control system for jam-absorption driving strategy against traffic waves in mixed traffic. *Applied Sciences*, 14(4), 1424.
- Muna, S.I., Mukherjee, S., Namuduri, K., Compere, M., Akbas, M.I., Molnár, P., and Subramanian, R. (2021). Air corridors: Concept, design, simulation, and rules of engagement. *Sensors*, 21(22), 7536.
- Pruekprasert, S. and Nakadai, S. (2025). Safe arrival scheduling at constraint waypoints in UAM corridors. In *Proc. of AIAA SciTech 2025 Forum*, 2232.
- Smith, N.M., Brasil, C., Lee, P.U., Buckley, N., Gabriel, C., Mohlenbrink, C.P., Omar, F., Parke, B., Speridakos, C., and Yoo, H.S. (2016). Integrated demand management: Coordinating strategic and tactical flow scheduling operations. In *Proc. of 16th AIAA Aviation Technology, Integration, and Operations Conference*, 4221.
- Thippavong, D.P., Apaza, R., Barmore, B., Battiste, V., Burian, B., Dao, Q., Feary, M., Go, S., Goodrich, K.H., Homola, J., et al. (2018). Urban air mobility airspace integration concepts and considerations. In *Proc. of 2018 Aviation Technology, Integration, and Operations Conference*, 3676.
- Vascik, P.D. and Hansman, R.J. (2018). Scaling constraints for urban air mobility operations: Air traffic control, ground infrastructure, and noise. In *Proc. of 2018 Aviation technology, Integration, and Operations conference*, 3849.
- Wang, Z., Delahaye, D., Farges, J.L., and Alam, S. (2021). Air traffic assignment for intensive urban air mobility operations. *Journal of Aerospace Information Systems*, 18(11), 860–875.
- Wing, D., Lacher, A., Ryan, W., Cotton, W., Stilwell, R., Maris, J., and Vajda, P. (2022). Digital flight: A new cooperative operating mode to complement VFR and IFR. URL <https://ntrs.nasa.gov/api/citations/20220013225/downloads/NASA-TM-20220013225.pdf>. Accessed: 2026-05-15.
- Wing, D.J., Prevot, T., Murdoch, J.L., Cabrall, C.D., Homola, J.R., Martin, L.H., Mercer, J.S., Hoadley, S.T., Wilson, S.R., Hubbs, C.E., et al. (2010). Comparison of airborne and ground-based function allocation concepts for nextgen using human-in-the-loop simulations. In *Proc. of 10th AIAA Aviation Technology, Integration and Operations (ATIO) Conference*, 9293.
- Yokoyama, N., Shindo, M., Matayoshi, N., and Yoshida, H. (2025). Performance evaluation of UATM services accounting for airspace and vertiport capacities. In *Proc. of AIAA SciTech 2025 Forum*, 2696.